Photoemission and Auger-electron spectroscopic study of the Chevrel-phase compound $Fe_xMo_6S_8$

A. Fujimori, M. Sekita, and H. Wada
National Institute for Research in Inorganic Materials, Sakura-mura, Niihari-gun, Ibaraki 305, Japan
(Received 23 October 1985)

The electronic structure of the Chevrel-phase compound $Fe_xMo_6S_8$ has been studied by photoemission and Auger-electron spectroscopy. Core-level shifts suggest a large charge transfer from the Fe atoms to the Mo_6S_8 clusters and a small Mo-to-S charge transfer within the cluster. Line-shape asymmetry in the core levels indicates that the density of states (DOS) at the Fermi level has a finite S $3p$ component as well as the dominant Mo $3d$ character. Satellite structure and exchange splitting in the Fe core levels point to weak Fe $3d$–S $3p$ hybridization in spite of the short Fe-S distances comparable to that in FeS. The x-ray and ultraviolet valence-band photoemission spectra and the Mo $4d$ partial DOS obtained by deconvoluting the Mo $M_{4,5}VV$ Auger spectrum are compared with existing band-structure calculations, and the Mo $4d$–S $3p$ bonding character, the structure of the Mo $4d$-derived conduction band etc., are discussed. In particular, it is shown that the conduction-band structure is sensitive to the noncubic distortion of the crystal through changes in the intercluster Mo $4d$–S $3p$ hybridization. A pronounced final-state effect is found in the Mo $M_{4,5}N_{2,3}V$ Auger spectrum and is attributed to strong $4p$-$4d$ intershell coupling.

I. INTRODUCTION

There has been considerable interest in the Chevrel-phase compounds $M_xMo_6X_8$ (M=Pb, Sn, Cu, rare-earth metals etc., and X=S, Se, or Te) which exhibit remarkable superconductive properties such as high superconductive transition temperatures T_c, high critical fields H_c, and weak depression of superconductivity by magnetic rare-earth ions.[1] These properties are supposed to arise from the electronic structure of these materials resulting from their unique crystal structures consisting of quasimolecular Mo_6X_8 clusters as shown in Fig. 1. The dependence of the structural stability on the valence electron number has also been discussed based on the gross electronic structure of the Mo_6X_8 cluster.[2,3]

Several theoretical studies including cluster calculations[4–6] and energy-band calculations[5–8] have been carried out. A typical density of states (DOS) (for $EuMo_6S_8$ calculated by Freeman and Jarlborg[8]) is shown in Fig. 2. According to these calculations, conduction-band levels within a few eV of the Fermi level E_F are derived predominantly from nonbonding Mo $4d$ states, and Mo $4d$–Xp bonding levels are formed about 3–8 eV below E_F. The Mo $4d$ conduction bands near E_F have very small dispersion giving rise to a high DOS and consequently high T_c and H_c[1]. The Mo $4d$–Xp antibonding levels are formed above E_F separated by a gap of 0–1 eV from the conduction bands. The principal role of the M atom is to distort the Mo_6X_8 host lattice and to donate electrons to the Mo- and X-derived energy levels.

Experimentally the electronic structures of $PbMo_6S_8$, $SnMo_6S_8$, $Cu_xMo_6S_8$ in the valence-band region have been studied by x-ray and ultraviolet photoemission spectroscopy (XPS and UPS)[9,10] and by x-ray emission spectroscopy.[10] While general agreement with the theoretical results mentioned above has been reported, several

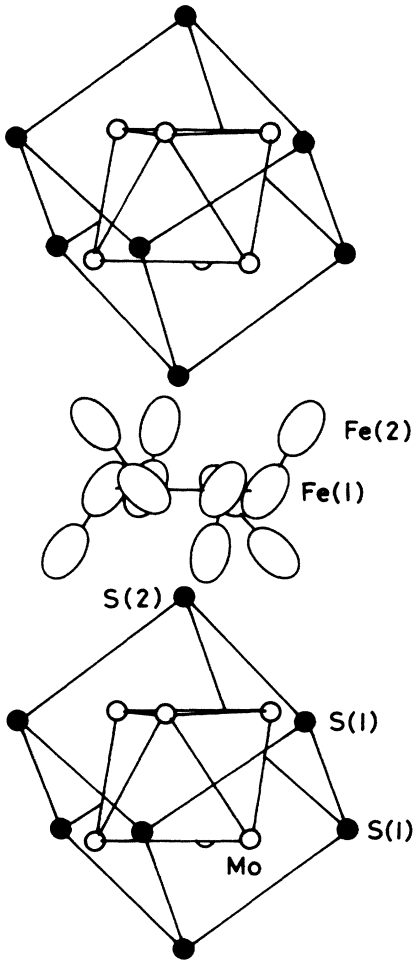

FIG. 1. Crystal structure of $Fe_xMo_6S_8$. Fe atoms statistically occupy two inequivalent sites, Fe(1) and Fe(2).

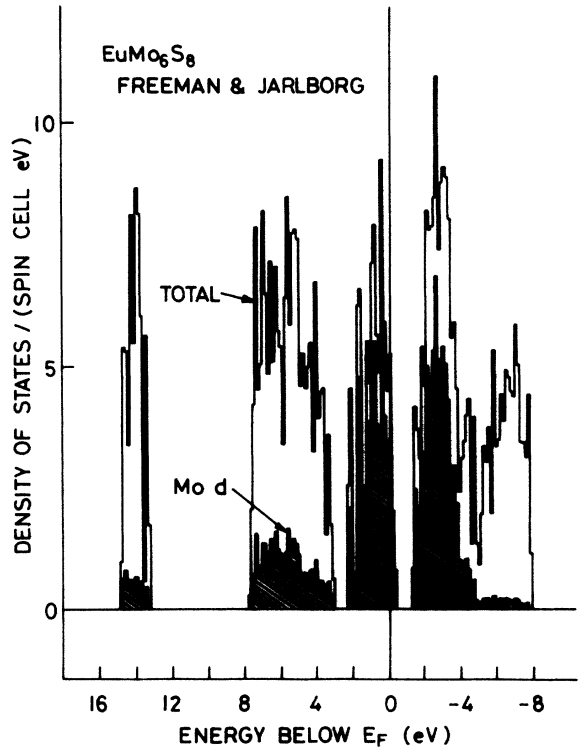

FIG. 2. Theoretical DOS of $EuMo_6S_8$ after a self-consistent LMTO band-structure calculation by Freeman and Jarlborg.[8]

discrepancies have been noted such as relative intensities of features in the bonding-level region,[10] a too deep experimental peak position of the Mo $4d$-derived conduction band,[10] and too low photoemission intensity at E_F^9. Furthermore, there are some disagreements between different band calculations[6-8] as for the positions and widths of the conduction band and Mo-S bonding bands. However, detailed comparison between theory and experiment has not been performed so far in order to clarify the above points.

In the present work, a Chevrel-phase compound $Fe_xMo_6S_8$ has been studied by XPS, UPS, and Auger-electron spectroscopy. In this material, superconductivity is destroyed by the magnetic Fe atoms.[1] Fe as well as Cu, Ni, etc., has small atomic radii as compared to Pb, Sn, rare-earth metals etc., and occupies different interstitial sites than the latter atoms (Fig. 1). The noncubic lattice distortion is thus different between these two types of $M_xMo_6S_8$ compounds (i.e., rhombohedral angle $\alpha > 90°$ for small M atoms and $\alpha < 90°$ for large M atoms).[11] In order to make an unambiguous comparison between experiment and theory, we took into account different cross sections for different atomic orbitals, instrumental and lifetime broadening, and a many-body line-shape function. It was found that the conduction-band structure is quite sensitive to the noncubic distortion mostly through the intercluster Mo $4d$—S $3p$ hybridization. Core-level XPS spectra were used to obtain information on the electronic structure through their binding-energy shifts, line shapes, satellite structures, and exchange splittings. Auger-electron spectroscopy was also utilized to obtain the local DOS at the Mo site.

II. EXPERIMENTAL

The samples were prepared by direct synthesis from stoichiometric mixture of FeS, MoS_2, and Mo powders sealed in quartz tubes. The products were then pressed into pellets having a diameter of 7 mm and were annealed at 1000 °C for 24 h. Two samples with compositions of $Fe_{1.25}Mo_6S_{7.75}$ and $Fe_{1.30}Mo_6S_{7.90}$, were obtained. The slight deficiency in the S content was necessary to produce single-phase materials.[12]

The XPS and Auger-electron spectra were excited by unmonochromatized Mg $K\alpha$ radiation ($h\nu = 1253.6$ eV) and the UPS spectra by He I ($h\nu = 20.1$ eV) and He II ($h\nu = 40.8$ eV) resonance lines. The emitted electrons were collected with a Physical Electronics 15-255 double-pass cylindrical mirror analyzer. Binding energies in XPS spectra have been calibrated with the Au $4f_{7/2}$ (84.0 eV) and Cu $2p_{3/2}$ (932.6 eV) core levels. Results for $Fe_{1.25}Mo_6S_{7.75}$ and $Fe_{1.3}Mo_6S_{7.9}$ are almost identical unless otherwise stated.

The samples were cleaned by scraping with a diamond file in the spectrometer chamber (base pressure in the 10^{-11} torr range). Even after extensive filing, a small amount of iron oxide ($\sim Fe_2O_3$) contamination could not be eliminated, but it did not increase under the vacuum for more than 10 h. Therefore, the contamination prob-

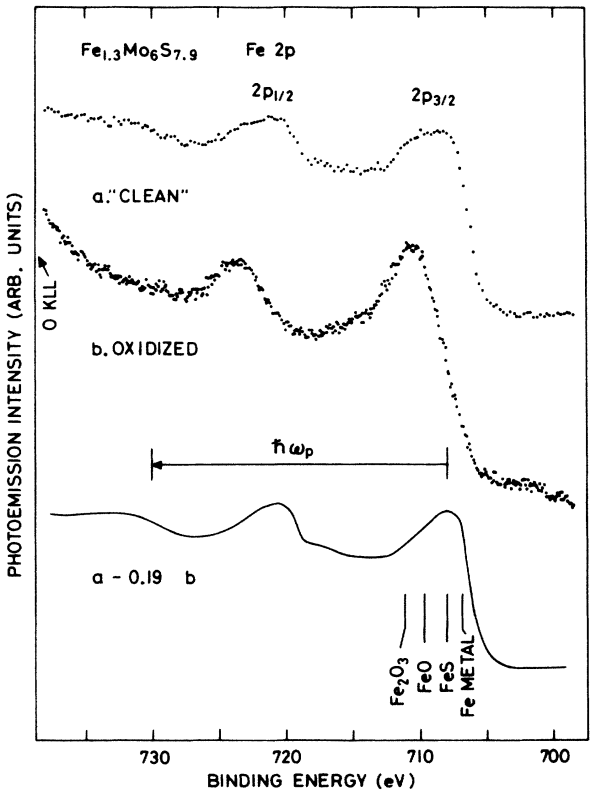

FIG. 3. Fe $2p$ core-level XPS spectrum of $Fe_{1.3}Mo_6S_{7.9}$ (bottom), which has been obtained by subtracting the contribution from iron oxide (oxidized in air) (middle) from the law data (top). The plasmon energy ($\omega_p \simeq 22.5 \pm 0.5$ eV) obtained from the energy loss peaks of the Mo and S core levels is shown. The $2p_{3/2}$ peak positions of Fe metal (Ref. 17) and various Fe compounds (Refs. 20 and 22) are also indicated.

ably arises from grain boundaries or pores of the sintered samples. From the core-level intensities,[13] approximately 20% of Fe atoms were found in the oxide form, while no sign of oxidation was seen in the Mo and S core levels. The oxide contribution in the Fe core levels, therefore, has been subtracted as shown in Fig. 3. This level of the iron oxide contamination is expected to be too low to affect the XPS and UPS valence-band spectra appreciably judged from the theoretical cross sections of Mo, 4*d*, S 3*p*, Fe 3*d*, and O 2*p* orbitals[14,15] except for weak, broad background emission.

Spectra shown in this paper have not been corrected for the electron kinetic energy dependence of the analyzer transmission, whereas theoretical, fitted curves for the valence-band and core levels have taken this dependence into account. The latter curves have also included the Mg $K\alpha_{3,4}$ ghost of the XPS radiation source.

III. RESULTS AND DISCUSSION

A. Core levels

From the empirical dependence of the structural stability on the valence electron number, it has been postulated that the *M* atoms donate electrons to the Mo_6S_8 clusters and that a Mo-to-S charge transfer occurs within the cluster.[1-3] The self-consistent linear-muffin-tin-orbital (LMTO) band calculations by Freeman and Jarlborg[8] have shown a charge transfer of 1—1.5 electrons from the *M* atom to the cluster. They have also shown that Mo in the Chevrel phase has ~4.5 *d* electrons and ~1.5 *sp* electrons, while Mo metal has ~5.1 *d* and ~0.9 *sp* electrons.[16] This means that electronic charges are less localized around the Mo cores in $M_xMo_6S_8$, since the *d* orbitals are spatially more localized than the *sp* orbitals. The non-self-consistent calculations by Nohl, Klose, and Andersen[7] have reached a similar conclusion. Such charge transfers can be tested by measuring core-level binding energy shifts.

The binding energies of the Mo, S, and Fe core levels and those in elemental solids are listed in Table I. The binding energy of Fe $2p_{3/2}$ is higher than that in Fe metal by ~1 eV, and agrees with FeS.[20] This suggests that the Fe atoms are in the divalent (Fe^{2+}:$3d^6$) configuration in $Fe_xMo_6S_8$, as Fe is divalent in FeS. Indeed, magnetic susceptibility measurements have shown that the Fe atoms in $Fe_xMo_6S_8$ are in the divalent and high-spin state.[21] However, the following differences are noted between FeS and $Fe_xMo_6S_8$: (i) the Fe 2*p* spectrum of $Fe_xMo_6S_8$ shows a weak feature at ~717 eV which might be assigned to a charge-transfer satellite accompanying the Fe $2p_{3/2}$ level (Fig. 3); (ii) the exchange splitting of the Fe 3*s* level ~5.7 eV (Fig. 4 and Table I) is much larger than that in the high-spin FeS, 4.4 eV,[20] or that in $Fe_{0.33}NbS_2$, in which Fe is also high-spin and divalent, 4.5 eV,[23] but is close to that in a highly ionic compound FeF_2, 6.0 eV.[24] The absence or weakness of the core-level satellites in the 3*d* transition-metal sulphides as compared to the oxides has been attributed to strong 3*d*—S 3*p* hybridization[25,26] or effects of itinerancy of 3*d* electrons.[27] The exchange splitting of the Fe 3*s* level has been found to be reduced by 3*d*-ligand hybridization in some compounds.[23,24] Therefore, the presence of the satellite and the large exchange splitting point to more ionic character in the Fe—S bond in $Fe_xMo_6S_8$ than in FeS. The weakness of the Fe-S hybridization may be supported by the large mobility of the Fe atoms[28] and by the oxidation study presented in Sec. III D. Fe is coordinated by six S atoms with the Fe-S distance of 2.46 Å in FeS and 2.42 Å in $Fe_{0.33}NbS_2$,[29] while in the rhombohedral phase of $Fe_xMo_6S_8$ by four S atoms with the Fe-S distance ranging from 2.3 to 2.6 Å.[30] (In FeS_2, where Fe is in the low-spin state due to strong Fe 3*d*—S 3*p* hybridization,[31] the Fe-S distance is 2.26 Å.) The weak Fe-S hybridization may partly be due to the smaller coordination number in $Fe_xMo_6S_8$. Also, the

TABLE I. Binding energies of core-level peaks in $Fe_xMo_6S_8$ compared with those in elemental solids (in eV).

		$Fe_xMo_6S_8$[a]	Elemental solids[b]
Mo	$4p_{3/2}$	35.8[c] (35.6)	35.5
	$4p_{1/2}$	(37.7)	37.6
	4*s*	62.8	63.2
	$3d_{5/2}$	228.1 (228.0)	227.9
	$3d_{3/2}$	231.3 (231.2)	231.1
S	$2p_{3/2}$	161.9[c] (161.7)	162.5
	$2p_{1/2}$	(162.9)	163.6
	2*s*	226.0	
Fe	3*s*	93.0, 98.7[d]	91.3, 95.3
	$2p_{3/2}$	708.2	706.8

[a]Numbers in parentheses are those obtained by least-squares fittings, and are generally different from the peak energies due to asymmetric broadenings or unresolved spin-orbit structures.
[b]Mo metal is from Ref. 17; solid S is from Ref. 18; Fe metal is from Refs. 17 and 19.
[c]Peak energy for the unresolved spin-orbit doublet.
[d]Two peaks are due to exchange splitting. Large errors are (±0.3 eV) expected from poor statistics.

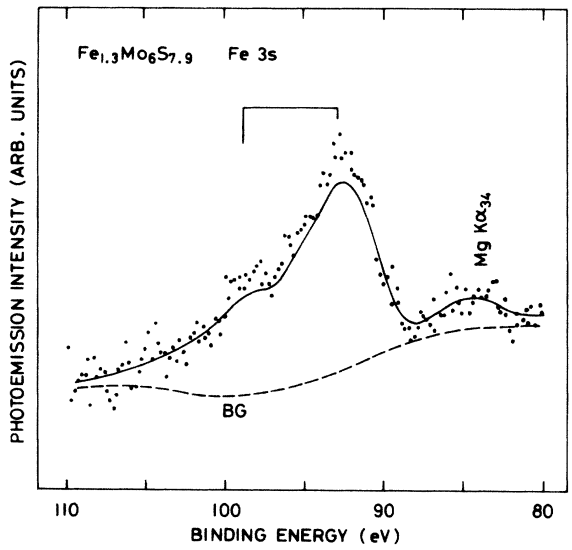

FIG. 4. Fe 3*s* core-level XPS spectrum of $Fe_{1.3}Mo_6S_{7.9}$ (solid curve). Contributions from iron oxide contamination have been subtracted from the raw data (dots) as in Fig. 3. A background due to the plasmon satellites of the Fe 3*p* and Mo 4*s* lines is shown by the dashed curve.

Mo-to-S charge transfer and/or the Mo-S hybridization might have resulted in weak Fe-S hybridization in spite of the short Fe-S distance. For M=Pb or Sn, the normal M-S(2) bonding has been suggested based on the normal M-S(2) distance,[3] which is consistent with the fact that S(1) is coordinated by four Mo atoms and S(2) by three Mo and one M atoms. From this argument the Fe-S(1) and Fe-S(2) distances would be expected to be systematically different, but this is not the case. Thus we suppose that the electronic interactions between the M atoms and the Mo_6S_8 clusters are weaker than would be expected from crystal chemistry consideration. In fact, band-structure calculations with and without M atoms have given quite similar results except for M-derived energy levels.[6]

The Mo core-level shifts relative to Mo metal, $\sim$0.3 eV, which are much smaller than in another metallic system MoO_2, $\sim$1.0 eV,[32,33] suggests only a small charge transfer from the Mo-to-S atoms. The S $2p$ level shifts to lower binding energies by $\sim$0.8 eV as compared to solid S. This shift, however, is partly due to metallic screening of the core hole (solid S is a semiconductor) and cannot be totally attributed to the charge transfer in the initial ground state.[34] Nevertheless, the S $2p$ binding energy is similar to that in metallic FeS (161.6 eV),[20] and would be consistent with the charge transfer from the Mo-to-S atoms.

In order to gain further information from the Mo and S core levels, we fitted the spectra to asymmetric line shapes given by Mahan[35] broadened with Gaussian and Lorentzian functions [full width at half maximum (FWHM) of $2G$ and 2γ, respectively]. The background due to inelastically scattered photoelectrons was assumed to be proportional to integrated photoemission intensity (excluding the background itself). The cutoff energy ξ (Ref. 35) was fixed at 4 eV, because this gave reasonable fits to all the core levels and the quality of the fits was not sensitive to small changes in ξ. The intensity ratio of the sin-orbit doublet was fixed to be the statistical ratio, while the lifetime widths were allowed to differ between the two lines in order to take into account the Coster-Kronig decay of the $j=l-\frac{1}{2}$ core hole into $l+\frac{1}{2}$. The different lifetime widths were necessary for each of the Mo $3d$ and $4p$ spin-orbit doublets as in Mo metal,[36] suggesting that Mo-derived empty levels are available about the spin-orbit splittings (3.2 eV and 2.1 eV for Mo $3d$ and $4p$, respectively) above E_F in order for the Coster-Kronig transition to occur. The $j=\frac{1}{2}$ and $\frac{3}{2}$ components of the S $2p$ level, on the other hand, were found to have the same lifetime widths within the uncertainty of the fitting procedure. This indicates that S-like states are not available about the S $2p$ spin-orbit splitting (1.2 eV) above E_F (i.e., the gap just above E_F may be larger than 1.2 eV or the S-derived DOS may be small for that excitation energy) or the transition matrix elements for the S $L_2L_3M_{2,3}$ Coster-Kronig process are small.

Figures 5 and 6 show the experimental and fitted spectra for the Mo $3d$ and S $2p$ core levels. The singularity indices as well as the lifetime and Gaussian widths are listed in Table II. According to Folmer and deBoer,[37] the singularity index α is proportional to the square of the local DOS at the core-hole site near E_F, if screening by only one atomic-orbital component at the core-hole site is considered. For the Mo core levels we obtained α=0.18, whereas α=0.12 has been obtained for Mo metal.[38] (As α is weakly dependent on the assumed ξ value, α=0.15 which was obtained by using the same ξ as that for Mo metal[38] should better be compared with the α of Mo metal.) Thus we conclude that the Mo $4d$ DOS around E_F in $Fe_xMo_6S_8$ is as high as or a little higher than that in Mo

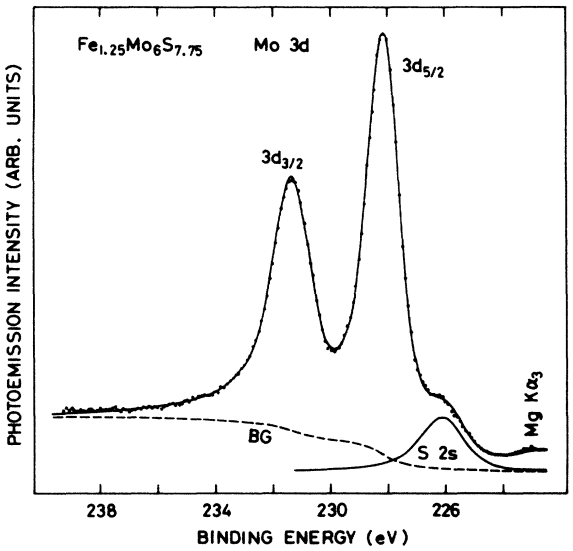

FIG. 5. Mo $3d$ core-level XPS spectrum of $Fe_{1.25}Mo_6S_{7.75}$. Data points have been fitted to a Mahan's asymmetric line shape (Ref. 35) (solid curve). The dashed curve represents the background.

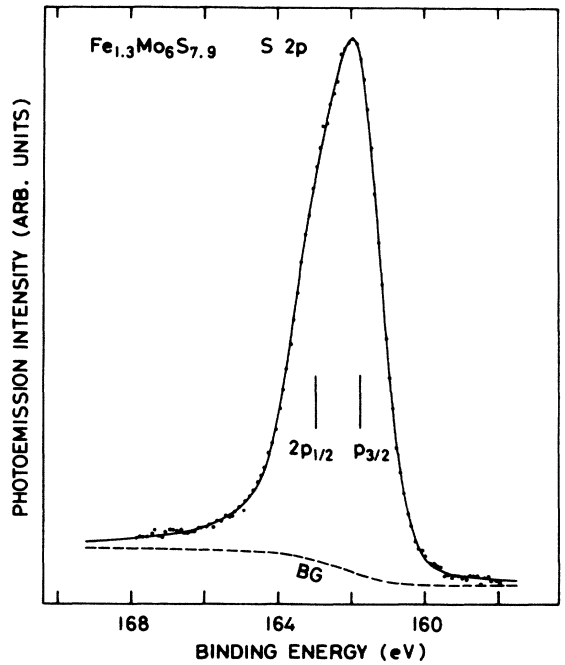

FIG. 6. S $2p$ core-level XPS spectrum of $Fe_{1.3}Mo_6S_{7.9}$ fitted to a Mahan's line shape as in Fig. 4.

TABLE II. Parameters for the line shapes of the Mo $3d$ and S $2p$ core levels in $Fe_{1.3}Mo_6S_{7.9}$. Energies are in eV.

	α	2γ $j=l+\frac{1}{2}$	2γ $j=l-\frac{1}{2}$	$2G$
Mo $3d$	0.18	0.48	0.72	0.98
Mo $4p$	0.16	1.14	1.62	1.51[a]
S $2p$	0.11	0.34[b]	0.34[b]	1.10

[a]Larger than that of Mo $3d$ because a larger pass energy was used.

[b]2γ's for $j=l+\frac{1}{2}$ and $l-\frac{1}{2}$ have been assumed to be the same.

metal, consistent with the band calculation results. The singularity index can also be given by[39]

$$\alpha=\sum_l q_l^2/2(2l+1)\ , \tag{1}$$

where q_l is the partial screening charge having an angular momentum l and satisfying the Friedel sum rule $\sum q_l=1$. If only Mo $4d$ electrons take part in the core-hole screening at the Mo site, we obtain from Eq. (1) $\alpha=0.1$, which is roughly consistent with the present result. The S $2p$ level also yields a finite α $(=0.11)$, implying finite S-derived DOS at E_F. In fact, the S $3p$–like DOS at E_F has been calculated to be finite i.e., 20–30% of the Mo $3d$ DOS.[7,8] Equation (1) gives $\alpha>0.125$ if the screening charges are restricted to s and p symmetry at the S site, but higher l components will reduce the lower limit. The cutoff energy $\xi=4$ eV used here is of the order of the average one-electron excitation energy within the Mo $4d$ DOS as can be seen from Fig. 2. Thus structures in the DOS (e.g., the gap just above E_F) are smeared out in the excitation spectrum as observed in the core-level line shapes as in other transition metals,[39] An asymmetric line shape itself is not always due to a finite DOS at E_F but may, in the case of semimetals, be due to an excitonic effect between the core hole and conduction electrons.[40] However, from the theoretical DOS, which have given finite Mo $4d$ and S $3p$ components at E_F, and its good agreement with experiment as shown below, it can be concluded *a posteori* that the symmetry is indeed due to the finite DOS at E_F and that the excitonic effect would not be important.

Although we have shown that the Fe $3d$–S $3p$ hybridization in the ground state is small in $Fe_xMo_6S_8$, it is not negligible. Indeed, the magnetic ordering[28] would be due to a superexchange interaction between the Fe ions mediated by the Mo_6S_8 clusters through the $3d$–S $3p$ hybridization. Thus the $3d$–S $3p$ hybridization is expected to result in a mixing of the Fe $3d$ character and consequently finite magnetic polarization at E_F, since the S $3p$ DOS has been found to be finite. (Direct Fe-Mo mixing would be less important because of the large Fe-Mo atomic distance, >3 Å.) This naturally explains the absence of superconductivity in $M_xMo_6X_8$ (M=Fe, Co, Ni, etc.). Such a mechanism should be extremely weak for M rare-earth metal because of the much weaker hybridization for the rare-earth $4f$ electrons.

B. Valence band

The valence-band spectra shown in Fig. 7 consist of three gross features at 0–2.5 eV, 2.5–9 eV, and 10–18 eV. The latter region is derived from the S $3s$ states. Considering the photon energy dependence of the atomic-orbital cross sections, namely rapid increase of the S $3p$ cross section below $h\nu\sim30$ eV with a Cooper minimum around $h\nu\sim50$ eV (Ref. 15) and relatively slow increase of the Mo $4d$ cross section below $h\nu\sim70$ eV and above $h\nu\sim100$ eV,[41] the former two regions can be assigned to Mo $4d$ nonbonding and Mo $4d$–S $3p$ bonding bands, respectively. This is consistent with the general electronic structure obtained by the various calculations[4–8] outlined in Sec. I. No photoemission features due to Fe $3d$ states have been identified in contrast to the Cu $3d$ emission in $Cu_xMo_6S_8$,[9,10] owing to low Fe concentration, low Fe $3d$ cross section,[14,15,42] and broad (~1 eV) energy spread of the final-state Fe $3d^5$ multiplet.[20,22]

In order to compare the band calculation results with the present spectra, the calculated DOS was convoluted with Gaussian, Lorentzian, and asymmetric[43] broadening functions, and backgrounds due to inelastically scattered electrons were assumed. The lifetime broadening of valence-band holes increases from ~0 at E_F toward higher binding energies, and we assumed a linear relation for the Lorentzian FWHM,[44]

$$2\gamma=2\gamma_0+a(E-E_F)\ . \tag{2}$$

Further, cross-section modulation effects due to the dif-

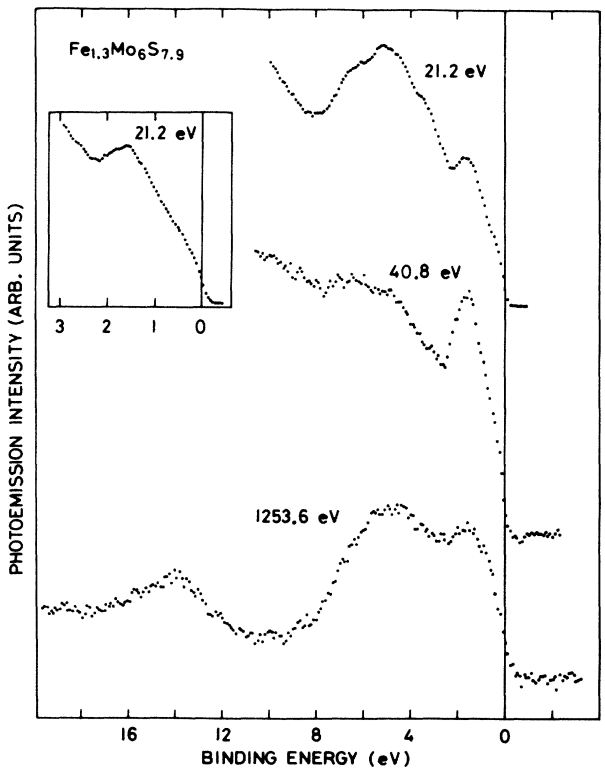

FIG. 7. Valence-band XPS and UPS spectra of $Fe_{1.3}Mo_6S_{7.9}$. In the insert, the He I ($h\nu=21.2$ eV) spectrum is shown in an expanded scale.

TABLE III. Parameters used to generate valence band photoemission spectra form theoretical DOS. Energies are in eV.

	α	$2\gamma_0$[a]	a	$2G$	Cross-section ratios S $3p$ to Mo $4d$	S $3p$ to S $3s$
XPS	0.14	0.14	0.18	0.51	0.8	0.6
He II	0.14	0.0	0.18	0.28	0.0	

[a]Nonzero for XPS due to the Lorenzian width of the unmonochromatized Mg $K\alpha$ radiation source.

ferent photon energy dependence of the Mo and S atomic orbital components were considered. Parameters used to generate theoretical valence-band spectra are listed in Table III. For XPS, the best resemblance to the experimental data was obtained by using a S $3p$ cross section which is larger than the theoretical cross section[14] by a factor of ~ 2. Similar enhancement has been observed for metal oxides[45] and hydrides,[46] and would be due to modification of the wave functions of the nonmetal atomic orbitals by chemical bonding or solid-state effects.

In Figs. 8 and 9, the valence-band spectra are compared with the three band-structure calculations: the calculations by Nohl, Klose, and Andersen (NKA)[7] for $PbMo_6S_8$ using the non-self-consistent LMTO method, by Freeman and Jarlborg (FJ)[8] for $EuMo_6S_8$ using the self-consistent LMTO method, and by Bullett[6] for Mo_6S_8 using an *ab initio* linear-combination-of-atomic-orbitals method (non-self-consistent).[47] (Bullett[6] has also presented the DOS of $PbMo_6S_8$, but its Mo $4d$ conduction band has been calculated to have too much weight near E_F to be compared with the present $Fe_xMo_6S_8$ spectra.) The noncubic distortion has not been included in the FJ calculations;[8] the result for $EuMo_6S_8$ and that for $SnMo_6S_8$ have given almost identical DOS (except for Sn- and Eu-derived states).[8] For each calculated DOS, the position of E_F has been corrected for the different electron numbers in $Fe_xMo_6S_{8-y}$ by assuming that an Fe atom or a S deficiency donates two electrons to the conduction band.

One can see in Figs. 8 and 9 general agreement between theory and experiment. As for the Mo-S bonding band, the NKA result is in good agreement with the experiment including the high-energy shoulder at 7 eV, while in Bullett[6] this shoulder has not been well reproduced. In the FJ result, on the other hand, the position of the bonding states as a whole is calculated to be too deep by as much

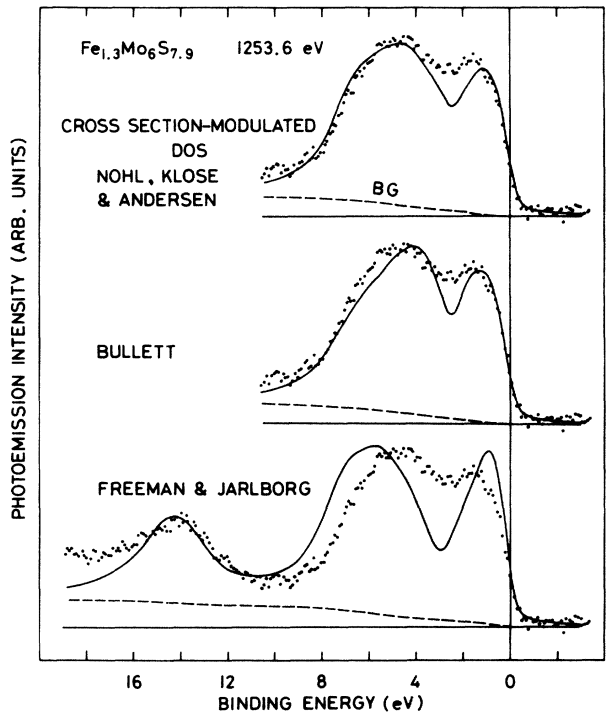

FIG. 8. Theoretical XPS valence-band spectra derived from the DOS by Nohl, Klose, and Andersen (Ref. 7), Bullett (Ref. 6), and Freeman and Jarlborg (Ref. 8) (solid curves) compared with experiment (dots). For broadening, background, and cross-section modulation, see the text and Table III.

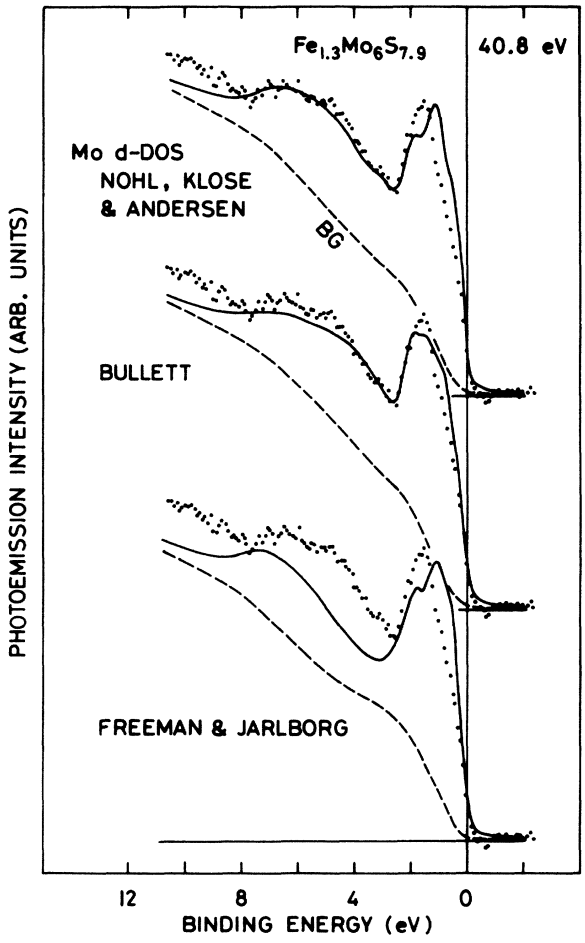

FIG. 9. Theoretical valence-band He II UPS spectra derived form the band calculations compared with experiment as in Fig. 8.

as ~ 1.5 eV. In a previous report Kurmaev *et al.*[10] noted disagreement between the self-consistent LMTO calculation and their XPS results, and attributed it to cross-section modulation effects rather than the energy positions. However, the LMTO result would not reproduce the experiment by using any Mo to S cross-section ratio, and we conclude that the energy positions have been calculated too deep.

The position of the Mo $4d$ conduction-band peak has been calculated to be too shallow in every calculation, among which the Bullett result for Mo_6S_8 has given the deepest peak position. Meanwhile, the photoemission spectra by Ihara and Kimura[9] have shown that the peak position is deeper for $Cu_xMo_6S_8$ than for $PdMo_6S_8$ and $SnMo_6S_8$.[9] As the rhombohedral angle decreases in the order of $Cu_xMo_6S_8$ ($\alpha \simeq 94.9°$), $Fe_xMo_6S_8$ ($\alpha \simeq 94.8°$), Mo_6S_8 ($\alpha \simeq 91.6°$), and $PbMo_6S_8$ ($\alpha = 89.2°$),[11] we may postulate that the conduction-band peak approaches E_F with decreasing rhombohedral angle. Thus the discrepancy in the conduction-band peak position between the experiment and the FJ or NKA result would largely be due to noncubic distortions different from that of $Fe_xMo_6S_8$. In fact, the peak position is in excellent agreement between NKA's result for $PbMo_6S_8$ and the UPS spectra[9] for $PbMo_6S_8$ (1.2 eV versus 1.1 eV).[48] No evidence for the reduction of the emission intensity at E_F was found as compared to the calculated DOS after properly taking into account various broadening effects.

The noncubic distortion may modify the Mo $4d$—derived conduction-band structure via (i) the direct Mo-Mo interaction, or (ii) the intracluster or intercluster Mo-S interaction. Changes in the intracluster Mo-Mo interaction would not be important because the intracluster Mo-Mo distances (in the range of 2.6–2.9 Å) do not vary within the compounds listed above to within ~ 0.02 Å (except for Mo_6S_8 where the Mo-Mo distance parallel to the rhombohedral axis is larger than in the other compounds by 0.1 Å). The intercluster Mo-Mo interaction would also be unimportant because the shortest intercluster Mo-Mo distance is as large as ~ 3.2 Å. Probably changes in the intracluster or intercluster Mo-S interaction with varying noncubic distortion are able to modify the conduction-band structure. The distortion of the Mo_6S_8 cluster from the cubic symmetry modifies significantly the energy levels around E_F (by 0.5–1 eV) via intracluster Mo-S interactions as has been suggested by Mattheiss and Fong[4] or shown by molecular-orbital calculations for cubic and distorted clusters by Bullett.[6] However, while the arrangement of the clusters changes with varying M atoms, the noncubic distortion of the cluster does not change and the effect of varying M atoms on the cluster structure is only to expand or contract differently the M_6 octahedron and the S_8 cube. The molecular-orbital calculations by Mattheiss and Fong[4] have shown that such a structural change is not important for the cluster energy-level structure. Therefore, changes in the intercluster Mo-S interaction seems to be the most important factor determining the conduction-band structure. The Mo d_{z^2} orbitals, which are directed toward neighboring clusters and thus should be sensitive to changes in the intercluster atomic distance, are about 1 eV below E_F in the cluster energy levels,[4–6] but are spread up to near E_F due to an intercluster banding effect.[7] Thus we suspect that changes in the intercluster Mo d_{z^2}—S $3p$ interaction are largely responsible for the changes in the Mo $4d$ conduction-band structure.

The existence of the gap ~ 2.5 eV below E_F between the conduction band and the bonding band is doubted at least for $Fe_xMo_6S_8$, as the valence band XPS shows extra intensity around 2.5 eV as compared to theory (Fig. 8). In particular, a gap of $\lesssim 1$ eV as calculated by FJ is too large for $Fe_xMo_6S_8$ and possibly for other $M_xMo_6S_8$ compounds.

There exist some differences between the spectra for $Fe_{1.3}Mo_6S_{7.9}$ and those for $Fe_{1.25}Mo_6S_{7.75}$. In the latter, the conduction-band peak is shallower than the former by 0.3 eV and the structures in the bonding levels at ~ 3.5 eV and ~ 7 eV are less pronounced. This would be related to the larger deviation of the Mo-S ratio from the stoichiometry $\frac{6}{8}$ due to S deficiency:[12] The Mo $4d$—S $3p$ bonding band is mainly derived from the S $3p$ states, and would therefore be sensitive to S defects. The conduction-band peak position would also be affected by S defects through intra- and inter-atomic Mo-S hybridization. (Difference in the position of E_F within the conduction band between the two samples is too small and is opposite to the observed shift, if an Fe atom or a S deficiency is assumed to donate two electrons to the conduction band.)

C. Auger-electron spectra

Auger transitions involving valence electrons can be used to probe local DOS at the core-hole site. In the case of a core-valence-valence (CVV) Auger transition, the spectrum reflects the DOS of two valence holes in the final state and, if correlation between the two holes can be neglected, i.e., if $U/W \ll 1$, where U is the Coulomb energy between the two holes at the same site and W is the bandwidth, it represents a self-convolution of the local DOS.[49] The Mo $M_{4,5}VV$ Auger spectrum has thus been self-deconvoluted by the method of Dose and Scheidt[50] and is shown in Fig. 10. The M_4VV/M_5VV intensity ratio is reduced from the statistical weight, $\frac{2}{3}$, owing to the M_4/M_5V Coster-Kronig transitions, and therefore was determined in a least-squares fitting way to be 0.14. In the figure, the deconvoluted spectrum is compared with the calculated Mo $4d$ partial DOS of NKA,[7] Bullett,[6] and FJ.[8]

From the reasonable agreement between the Mo $4d$ DOS and the deconvoluted spectrum, one can say that the $M_{4,5}VV$ spectrum involves largely Mo $4d$ electrons with a negligible Mo sp contribution and that the two valence holes are not strongly correlated. The latter conclusion is consistent with the valence-band photoemission spectra which have been reasonably compared with the one-electron DOS. This is also consistent with the absence of strong many-body effects in the low-energy scale such as mass enhancement near E_F.[1,51] Calculations by Tréglia *et al.* on CVV Auger spectra for partially filled d bands[52] have shown that the spectra deviate appreciably from a self-convolution when $U/W \gtrsim 0.1$. Therefore, an upper

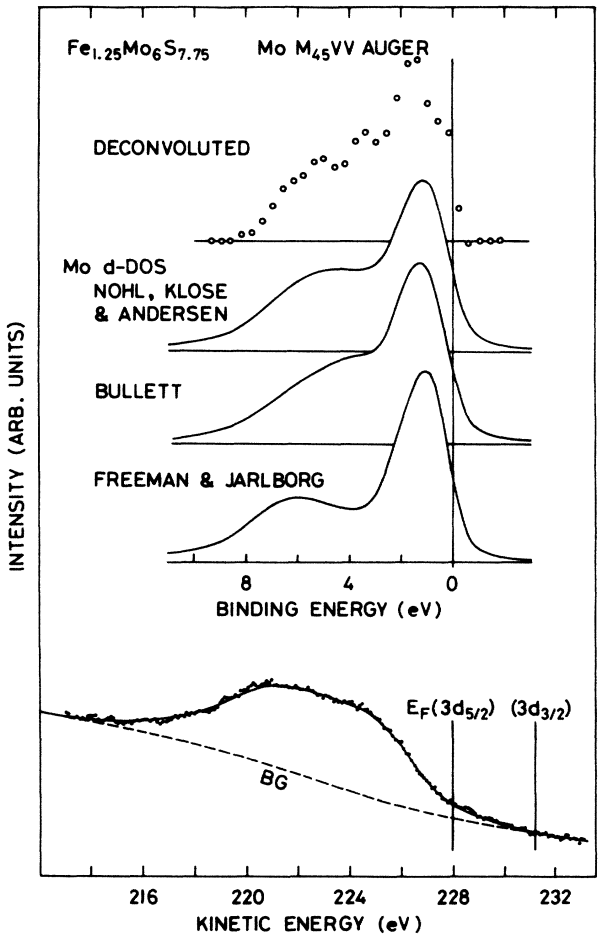

FIG. 10. Mo $M_{4,5}VV$ Auger spectrum of $Fe_{1.25}Mo_6S_{7.75}$ (bottom) and its self-deconvolution (top) compared with the theoretical Mo 4*d* partial DOS. The DOS has been broadened with the lifetime broadening of the Mo $3d_{5/2}$ core-level and valence holes and a Gaussian resolution function ($2G \sim 0.8$ eV). The solid curve superimposed on the spectrum shows the self-convolution of the top panel.

limit of ~ 1 eV would be set for U, as the relevant bandwidth would be between ~ 6 eV (the nonbonding plus antibonding bands) and ~ 12 eV (including the bonding band also).

As in the case of the valence-band photoemission, one can see from Fig. 10 that the position of the Mo 4*d*—S 3*p* bonding band is in good agreement with the NKA (Ref. 7) and Bullett (Ref. 6) results and the peak position of the Mo 4*d* conduction band with the Bullett result.[6] The bonding band of FJ is again too deep, and its intensity is a little too low. The latter fact indicates that the Mo 4*d* character in the bonding band is calculated to be too small in the FJ results, suggesting a too ionic character in the Mo—S bond. Although self-consistent calculations do not always give DOS in better agreement with experiment than non-self-consistent calculations (for example see Refs. 46 and 53), self-consistent calculations are expected to give more reliable charge distribution and consequently more reliable ionic-versus-covalent character of chemical bonds. The simplified crystal structure in the FJ calculation may be responsible for the above discrepancy, as lowered symmetry causes further Mo 4*d*—S 3*s* hybridization which is not allowed in the cubic phase, but the discrepancy seems too large to be explained only by the crystal distortion. This may be due to the limit of approximations made in the LMTO method or of the local-density approximation itself.

Figure 11 shows two types of core-core-valence Auger transitions, namely the Mo $M_{4,5}N_1V$ and $M_{4,5}N_{2,3}V$ Auger spectra, compared with the convoluted Mo 4*d* partial DOS. In a one-electron picture, these spectra are given by a partial DOS at the Mo site. This was in fact found to be the case for the $M_{4,5}N_1V$ transition as demonstrated by a good fit to the convoluted Mo 4*d* DOS shown in Fig. 11. In contrast to the $M_{4,5}N_1V$ spectrum, the $M_{4,5}N_{2,3}V$ spectrum could not be fitted to a convoluted DOS in any way: Intense extra emission on the low kinetic energy side is evident from the figure. As initial-state effects (screening of the initial-state core hole)[54] would be negligible because of their absence in the Mo $M_{4,5}VV$ spectrum, the anomalous $M_{4,5}N_{2,3}V$ spectrum is probably due to final-state effects. Thus we can attribute the anomaly to a modification of the valence-hole spectrum or formation of a splitoff localized valence hole by the final-state core-hole potential.[55,56] However, simple spherically symmetric core-hole potentials alone cannot explain the experimental results, since the 4*s* and 4*p* hole potentials are expected to be similar. Therefore, we postulate that the multiplet coupling of the 4*p* core hole with the 4*d* valence hole is responsible for the final-state effect. The strong 4*p*-4*d* multiplet coupling, if it exists, is due to a large dipole-type exchange interaction represented by a Slater integral $G_1(4p,4d)$, which is expected to be of the order of a few tenths eV from those in other elements,[57,58]

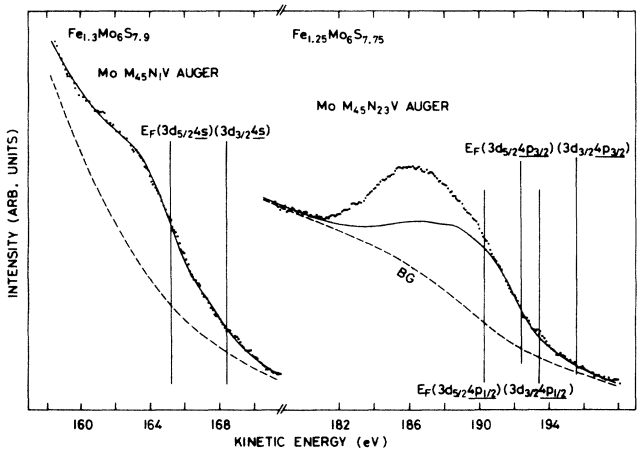

FIG. 11. Mo $M_{4,5}N_1V$ and $M_{4,5}N_{2,3}V$ Auger spectra of $Fe_xMo_6S_8$. The solid curves are convolutions of the Mo 4*d* partial DOS which take into account the lifetime widths of the Mo N_1 (4*s*), $N_{2,3}$ (4*p*), and $M_{4,5}$ (3*d*) core levels. The statistical N_2-N_3 ratio (0.5) has been assumed, while the $M_4N_{2,3}V$-$M_5N_{2,3}V$ and M_4N_1V-M_5N_1V ratios have been determined to be 0.10 and 0.30, respectively. For the $M_{4,5}N_1V$ spectrum, in addition to the background which is proportional to the integrated Auger emission intensity, a parabolic component was assumed in order to represent the rapid rise toward lower kinetic energies.

and would produce a multiplet splitting of the order of several eV. The $4s$-$4d$ multiplet splitting is expected to be about half of the spread of the $4p$-$4d$ multiplet,[59] and may not be large enough to split off localized states from the bandlike states. To make a more definitive conclusion, the intensities of the multiplet lines should be known for partially filled, itinerant d bands, but such calculations have not been performed so far.

D. Surface oxidation

The clean surfaces of $Fe_xMo_6S_8$ were fairly stable against oxidation as can be seen from the O $1s$ core signal intensity which remained constant for a long time under the vacuum of the spectrometer. Oxidation of $Fe_{1.3}Mo_6S_{7.9}$ was carried out by exposing the clean surface to air for a few minutes. Resulting Mo and S core-level spectra are shown in Fig. 12. The Fe $2p$ core level of the oxidized surface is shown in the middle panel of Fig. 3. From these figures one can see that most of the Fe atoms within the escape depth λ of photoelectrons are oxidized to Fe^{3+} ($\sim Fe_2O_3$) while Mo and S atoms remain mostly unoxidized: A weak signal of oxidized Mo ($\sim MoO_3$) is discernable in Fig. 12, but not for S. Effects of oxidation become more evident in UPS due to smaller electron escape depths: The He II spectra ($\lambda \sim 4$ Å) have indicated a buildup of O $2p$ emission at 3–10 eV and reduction of the Mo $4d$ conduction-band emission by a factor of ~ 0.3, suggesting oxidation of the Mo atoms (formation of MoO_3-like oxide) near the surface. As for the XPS valence band, where the escape depth is a few ten Å, the only change upon oxidation is a slight increase of emission intensity around 3–10 eV probably due to O $2p$ and Fe $3d$ emission.

It is surprising that even such a heavy exposure is far from oxidizing Mo atoms completely. It seems that the Mo_6S_8 clusters are chemically quite inert analogous to the layered structure MoS_2.[60] The S atoms are particularly inert as can be seen from the core levels. This is consistent with the conclusion drawn from the Fe core-level spectra in Sec. III A that the Fe $3d$–S $3p$ hybridization is weak.

IV. CONCLUSION

The valence band and core levels of the Chevrel-phase compound $Fe_xMo_6S_8$ have been studied by photoemission and Auger-electron spectroscopy. The core-level shifts suggest a large charge transfer from the Fe atoms to the Mo_6S_8 clusters and a small Mo-to-S charge transfer within the cluster. Core line-shape asymmetry indicates that the DOS at E_F has a finite S $3p$ component as well as the dominant Mo $4d$ component. Thus conduction electrons are partially polarized via Fe $3d$–S $3p$ hybridization, resulting in the depression of superconductivity. The satellite structure in the Fe $2p$ core level and the magnitude of the exchange splitting in the Fe $3s$ core level indicate that the Fe $3d$–S $3p$ hybridization is weak in spite of the Fe-S distance as short as that in FeS where stronger Fe $3d$–S $3p$ hybridization exists. This is supported by the oxidation study and is consistent with the high mobility of the Fe atoms and the structural properties. The XPS and UPS valence-band spectra and the Mo $4d$ partial DOS obtained by deconvolution of the Mo $M_{4,5}VV$ Auger spectrum are compared in detail with existing band-structure calculations by taking into account appropriately various broadening effects and backgrounds. Satisfactory agreement is obtained with the theoretical DOS including the DOS at E_F, although the self-consistent LMTO calculations seem to lead to somewhat too much ionic character in the Mo $4d$—S $3p$ bond. The Mo $4d$–derived conduction band near E_F is shown to be sensitive to noncubic distortion of the crystal, which depends on the size of the M atom in $M_xMo_6S_8$ and real crystal structures are found to be necessary to calculate correctly the conduction-band structure. The anomalous line shape of the Mo $M_{4,5}N_{2,3}V$ Auger spectrum is attributed to a final-state effect, namely strong $4p$-$4d$ intershell Coulomb-exchange interactions.

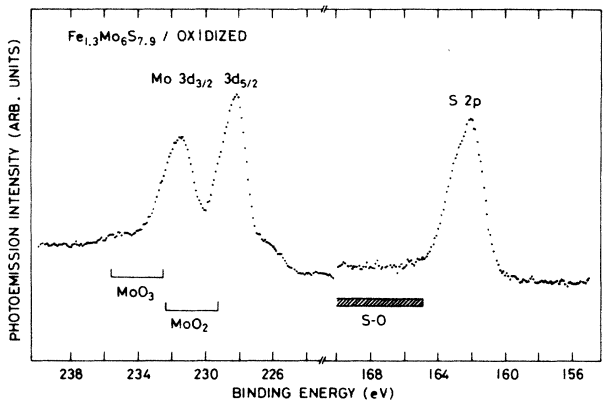

FIG. 12. Mo $3d$ and S $2p$ core-level XPS spectra for $Fe_{1.3}Mo_6S_{7.9}$ oxidized by exposing the clean surface to air. Peak positions for molybdenum oxides and sulpher-oxygen compounds (e.g., Na_2SO_3) are indicated. Note a weak signal corresponding to MoO_3 and the absence of any sign of oxidization for the S $2p$ core level. The Fe $2p$ core level for the same surface is shown in Fig. 3.

ACKNOWLEDGMENTS

We would like to acknowledge useful discussions with Dr. I. Kawada, Dr. H. Nozaki, Dr. N. Kimizuka, Dr. H. Ihara, and Professor S. Suga.

[1]For review, see, e.g., *Superconductivity in Ternary Compounds*, edited by Ø. Fischer and M. B. Maple (Springer-Verlag, Berlin, 1982), Vols. I and II; Ø. Fisher, Appl. Phys. **16**, 1 (1978).

[2]K. Yvon and A. Paoli, Solid State Commun. **24**, 41 (1977).

[3]K. Yvon, in *Superconductivity in Ternary Compounds I*, edited by Ø. Fischer and M. B. Maple (Springer-Verlag, Berlin, 1982), p. 87.

[4]L. F. Mattheiss and C. Y. Fong, Phys. Rev. B **15**, 1760 (1977).

[5]O. K. Andersen, W. Klose, and H. Nohl, Phys. Rev. B **17**, 1209 (1978).
[6]D. W. Bullett, Phys. Rev. Lett. **39**, 664 (1977).
[7]H. Nohl, W. Klose, and O. K. Andersen, *Superconductivity in Ternary Compounds I*, Ref. 3, p. 185.
[8]T. Jarlborg and A. J. Freeman, Phys. Rev. Lett. **44**, 178 (1980); A. J. Freeman and T. Jarlborg, in *Superconductivity in Ternary Compounds II*, edited by M. B. Maple and Ø. Fischer (Springer-Verlag, Berlin, 1982), p. 167.
[9]H. Ihara and K. Kimura, Jpn. J. Appl. Phys. **17**, Suppl. 17-2, 281 (1978).
[10]E. Z. Kurmaev, Y. M. Yamoshenko, R. Nyholm, N. Mårtensson, and T. Jarlborg, Solid State Commun. **37**, 647 (1981).
[11]R. Chevrel and M. Sergent, *Superconductivity in Ternary Compounds I*, Ref. 3, p. 25.
[12]H. Wada, M. Onoda, H. Nozaki, and I. Kawada, J. Less-Common Met. **113**, 53 (1985).
[13]Estimated by using the theoretical cross section (Ref. 14) corrected for kinetic-energy-dependent electron mean-free paths [D. R. Penn, J. Electron Spectrosc. Relat. Phenom. **9**, 29 (1976)] and analyzer transmission [P. W. Palmberg, J. Vac. Sci. Tech. **12**, 379 (1975)]. It has been assumed that the oxygen signal originates from the iron oxide part on the surface and not from a thin surface oxide layer.
[14]J. H. Scofield, J. Electron Spectrosc. Relat. Phenom. **8**, 129 (1976).
[15]D. J. Kennedy and S. T. Manson, Phys. Rev. A **5**, 227 (1972).
[16]D. G. Pettifor, J. Phys. F **7**, 613 (1977).
[17]J. C. Fuggle and N. Mårtensson, J. Electron Spectrosc. Relat. Phenom. **21**, 275 (1980); in this reference, binding energies have been calibrated in the same way as in the present work to within ±0.1 eV.
[18]W. R. Salaneck, N. O. Lipari, A. Paton, R. Zallen, and K. S. Liang, Phys. Rev. B **12**, 1493 (1975).
[19]J. Azouley and L. Ley, Solid State Commun. **31**, 131 (1979).
[20]J. Gopalakrishnan, T. Murugesan, M. S. Hedge, and C. N. R. Rao, J. Phys. C **12**, 5255 (1979).
[21]H. Nozaki, H. Wada, and I. Kawada (unpublished).
[22]C. R. Brundle, T. J. Chuang, and K. Wandelt, Surf. Sci. **68**, 459 (1977).
[23]J. J. Barry and H. P. Hughes, J. Phys. C **16**, L275 (1983).
[24]J. C. Carver, G. K. Schwetzer, and T. A. Carlsson, J. Chem. Phys. **57**, 973 (1972); results for FeS in this reference are quite different from those in Ref. 20 probably due to surface contamination.
[25]D. D. Sarma, P. Vishnu-kamath, and C. N. R. Rao, Chem. Phys. **73**, 71 (1983).
[26]S. Larsson and M. Lopes de Siqueria, Chem. Phys. Lett. **44**, 537 (1976).
[27]S. Asada and S. Sugano, J. Phys. C **11**, 3911 (1978).
[28]J. M. Friedt, C. W. Kimball, A. T. Aldred, B. D. Dunlap, F. Y. Fradin, and G. K. Shenoy, Phys. Rev. B **29**, 3863 (1984).
[29]W. B. Clark, J. Phys. C **9**, L693 (1976).
[30]P. J. Guillevic, O. Bars, and D. Grandjean, Acta Crystallogr., Sect. B **32**, 1338 (1976).
[31]P. Burgart and M. S. Seehra, Solid State Commun. **22**, 153 (1977).
[32]K. S. Kim, W. E. Baitinger, J. W. Amy, and N. Winograd, J. Electron Spectrosc. Relat. Phenom. **5**, 351 (1974).
[33]F. Werfel and E. Minni, J. Phys. C **16**, 6091 (1983).
[34]A comparable shift (~1 eV) has been observed for the S $2p$ core level between semiconducting CaS and metallic ScS [H. F. Franzen, M. X. Umaña, J. R. McCreary, and R. J. Thorn, J. Solid State Chem. **18**, 363 (1976)].
[35]G. D. Mahan, Phys. Rev. B **11**, 4814 (1975).
[36]N. Mårtensson and R. Nyholm, Phys. Rev. B **24**, 7121 (1981).
[37]J. C. W. Folmer and D. K. G. deBoer, Solid State Commun. **38**, 1135 (1981).
[38]H. Höchst, P. Steiner, G. Reiter, and S. Hüfner, Z. Phys. B **42**, 199 (1981).
[39]G. K. Wertheim and P. H. Citrin, in *Photoemission in Solids*, edited by M. Cardona and L. Ley (Springer-Verlag, Berlin, 1978), Vol. I, p. 197.
[40]P. M. Th. M. van Attekum and G. K. Wertheim, Phys. Rev. Lett. **43**, 1986 (1979).
[41]I. Abbati, L. Braicovich, C. Carbone, J. Nogami, J. J. Yeh, I. Lindau, and U. del Pennio, Phys. Rev. B **32**, 5459 (1985).
[42]The total Fe $3d$ emission intensity would be only about 5% of the valence-band emission in XPS, taking into account the enhancement of the S $3p$ cross section discussed in the text, and would also be small in UPS.
[43]It has been shown in Ref. 38 that the valence-band spectra of $4d$ transition metals can be well reproduced by convoluting the theoretical DOS with asymmetric line-shape functions having the same singularity indices as those of the core levels.
[44]A. Fujimori and F. Minami, Phys. Rev. B **30**, 957 (1984).
[45]G. A. Sawatzky and D. Post, Phys. Rev. B **20**, 1546 (1979).
[46]A. Fujimori and L. Schlapbach, J. Phys. C **17**, 341 (1984).
[47]In Bullet (Ref. 6), only the total DOS is given. Therefore, we scaled the DOS in the conduction-band and bonding state regions by different factors in order to simulate relative changes of the Mo $4d$ and S $3p$ cross sections. This would be justified because in each region the partial DOS's have similar shapes (see Fig. 2).
[48]The conduction-band peak in the XPS spectrum of $PbMo_6S_8$ by Kurmaev *et al.* (Ref. 10) is too deep (~2 eV below E_F). The cause for such a large discrepancy is not clear; a part of this discrepancy could be due to possible inaccurate determination of E_F in their XPS measurements.
[49]M. Cini, Solid State Commun. **24**, 681 (1977); G. A. Sawatzky, Phys. Rev. Lett. **39**, 504 (1977).
[50]V. Dose and H. Scheidt, Appl. Phys. **19**, 19 (1979).
[51]Enhancement in the specific heats is largely explained by electron-phonon interaction as deduced from T_c^1, and extra enhancement is 1–1.5. If one compares the calculated DOS at E_F and the specific heats, the enhancement factors are 1–1.7.
[52]G. Tréglia, M. C. Desjonquères, F. Ducastelle, and D. S. Spanjaard, J. Phys. C **14**, 4347 (1981).
[53]D. J. Peterman, J. H. Weaver, and D. T. Peterson, Phys. Rev. B **23**, 3903 (1981).
[54]D. R. Jennison, H. H. Madden, and D. M. Zehner, Phys. Rev. B **21**, 430 (1980); M. Davies, D. R. Jennison, and P. Weightman, *ibid.* **29**, 5313 (1984).
[55]U. von Barth and G. Grossmann, Solid State Commun. **32**, 645 (1979).
[56]R. Lässer and J. C. Fuggle, Phys. Rev. B **22**, 2637 (1980).
[57]T. Yamaguchi, S. Shibuya, and S. Sugano, J. Phys. C **15**, 2625 (1982).
[58]A. Fujimori, J. H. Weaver, and A. Franciosi, Phys. Rev. B **31**, 3549 (1985).
[59]Inferred from the $3p^5 3d^9$ and $3s^1 3d^9$ multiplets in Cu, see J. F. McGilp and P. Weightman, J. Phys. C **11**, 643 (1978).
[60]J. C. Menamin and W. E. Spicer, Phys. Rev. B **16**, 5474 (1977).